RELATIONSHIP OF GAUSSIAN BEAM THEORY TO SCANNED ULTRASONIC MEASUREMENTS WITH COMMERCIAL TRANSDUCERS

R. B. Thompson and E. F. Lopes

Ames Laboratory
Iowa State University
Ames, IA 50011

INTRODUCTION

The effects of diffraction play an important role in defining the performance of an ultrasonic inspection. For example, in a scanned inspection with a focussed probe, diffraction determines the size of the beam near the focal point. This in turn defines the size of the scan increments which will produce a desired probability of detecting a flaw. Increments which are too great will introduce a greater possibility of missing a flaw. Those which are too small will cause excess time and inspection cost.

The patterns of the radiation of piston sources into a fluid are well known (1). However, even in this simple case, numerical techniques must be employed to evaluate the off-axis fields except in the true far field. After such a beam propagates through a curved interface at oblique incidence, the situation becomes considerably more complex, and even the evaluation of the axial fields must be done numerically (2).

On the other hand, for a transducer with a Gaussian profile, these problems become much simpler. Within the scalar, Fresnel approximation, analytical expressions have been developed which predict the fields at all points in space (3). These solutions are of interest in themselves because of the absence of side lobes in Gaussian beams and increasing efforts to make them practically realizable (4-6). However, the present work adopts a slightly different philosophical point of view. It is suggested herein that, by properly selecting the parameters of a Gaussian beam, one can develop a simple theory which will describe, in a semi-quantitative fashion, the behavior of the central lobe of the radiation of a piston transducer near a focal point. This may be an attractive tool in the initial design of scanned ultrasonic systems.

REVIEW OF GAUSSIAN BEAM THEORY

The theory of scalar, Gaussian beams, as it applies to ultrasonic measurements, has been recently described in detail (3). Here only

the final "recipe" will be reproduced. Figure 1 illustrates the geometry of interest. A Gaussian transducer is assumed to illuminate a cylindrical interface, with oblique incidence in the x-z plane. The (x_o,y_o,z_o) coordinate system is assumed to have its origin at the transducer face, its z_o-axis along the central ray of the beam, its y_o-axis perpendicular to the plane of the figure, and its x_o-axis in the appropriate orthogonal direction in the plane of the figure. The (x,y,z) coordinate system has its origin at the point of intersection of the central ray with the curved interface. The z_1-axis coincides with the refracted central ray. The y_1-axis is again perpendicular to the plane of the figure and the x_1-axis is rotated appropriately. The interface is assumed to have a radius of curvature B.

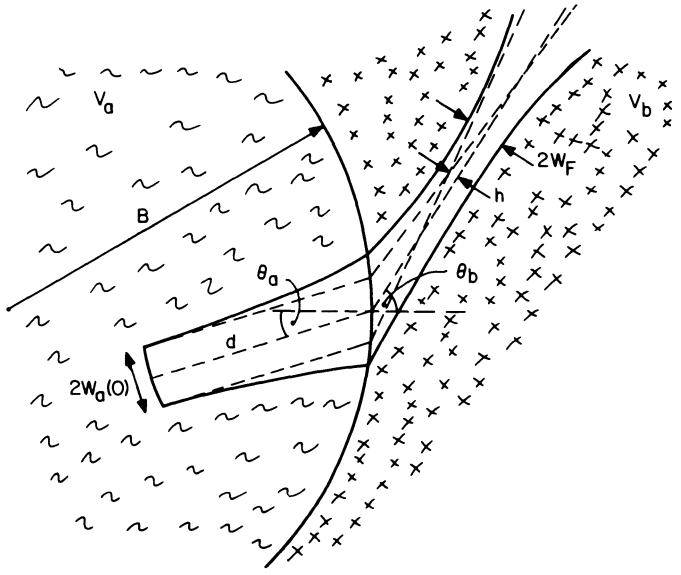

Fig. 1. Geometry of interface transmission problems.

Let ϕ be the acoustic velocity potential, which is assumed to have the value at the transducer of

$$\phi(x_o,y_o,0) = \phi_o \exp[-(x_o^2+y_o^2)/w_o^2 - j\pi(x_o^2+y_o^2)/\lambda R_o] \quad (1)$$

where ϕ_o is a constant amplitude, w_o is the half-width of the Gaussian, and R_o is the radius of curvature of the wavefronts. In this sign convention, the beam is converging for $R_o<0$ and diverging for $R_o>0$. The theory of scalar, Gaussian beams, indicate that the fields at other points in the fluid are then given by

$$\phi(x,y,z) = A\left(\frac{w(o)}{w(z)}\right) \exp\{j[\psi(z)-\psi(o)-kz - k(x^2+y^2)/2q(z)]\} \quad (2)$$

where

$$q(z) = q(o) + z \quad (3)$$

$$\frac{1}{q(o)} = \frac{1}{R(o)} - \frac{j\lambda}{\pi w(o)^2} \quad (4)$$

$$w(z) = \left[\frac{-\lambda/\pi}{Im(1/q)}\right]^{\frac{1}{2}} \quad (5)$$

$$\psi(z) = \pi/2 - \angle q(z) \quad (6)$$

$$R(z) = \frac{1}{Re(1/q(z))} \quad (7)$$

Here q(z) may be thought of as a generalized radius of curvature whose imaginary part describes the diffraction induced modifications of the propagation laws of geometrical acoustics (q becomes real as $\lambda \to 0$), w(z) and R(z) are the beam width and radius of phase curvature and $\psi(z)$ is a slowly varying phase factor. A simple generalization of the above to elliptical beams is discussed elsewhere (3).

The essential feature of the Gaussian beam theory is that the evolution of the fields during propagation, e.g., focussing and/or beam spread, are fully defined by the complex parameter q, which changes linearly with distance as specified by Eq. (3). Specification of q at any plane fully defines the beam at subsequent planes. Because of this simplicity, propagation through an interface is introduced into the theory by a transformation of q,

$$\begin{pmatrix} q_T^{-1} \end{pmatrix} = \frac{V_b}{V_a}\frac{Cos^2\theta_a}{Cos^2\theta_b}\begin{pmatrix} q_I^{-1} \end{pmatrix} - \begin{pmatrix} [V_b Cos\theta_a/V_a - Cos\theta_b]/BCos^2\theta_b \\ 0 \end{pmatrix} \quad (8)$$

where the various symbols are defined in Fig. 1. Recalling that q may be thought of as a generalized radius of curvature, Eq. (8) represents the fact that wavefront curvatures change at the interface due to both refraction (first term) and focussing if the interface is curved (second term). Note that Eq. (8) is a matrix equation in which the upper element corresponds to the real part and the lower element to the imaginary part of the indicated quantity. This should not be confused with a spatial vector.

After propagation through a cylindrical or bi-cylindrical interface, or a planar interface at oblique incidence, the radiation pattern in the x_1-y_1 plane will differ from that in the y_1-z_1 plane. Because of the separability of the Gaussian beam theory in x and y, these characteristics can be treated independently. The solution in the solid is then

$$\phi(x,y,z) = A_b \left[\frac{w_x(o)}{w_x(z_1)}\right]^{\frac{1}{2}} \left[\frac{w_y(o)}{w_y(z_1)}\right]^{\frac{1}{2}} \exp\{j[\psi_x(z_1)+\psi_y(z_1)-\psi_x(o)-\psi_y(o)-kz_1]\}$$

$$\exp\{-j\ [\ kx_1^2/2q_x + ky_1^2/2q_y]\} \qquad (9)$$

where Eqs. (4)-(7) are separately applied to the propagation in the x_1-z_1 and y_1-z_1 planes (3). In addition, Eq. (6) must be modified to the form $\psi_{x,y}(z_1) = 0.5\ (\pi/2 - \angle q_{x,y}(z_1))$ so that the proper limit is retained when the x_1 and y_1 directions are equivalent. In order to ensure that the displacement has the proper continuity at interfaces, the overall amplitude of the scalar potential must transform in accordance with the relation.

$$A_b = \frac{V_b}{V_a} T_{ab} A \left[\frac{w_o}{w(z_o=d)}\right] \exp\{j[\psi_x(d)+\psi_y(d)-\psi_x(o)-\psi_y(o)-kd]\} \qquad (10)$$

where T_{ab} is the liquid-solid transmission coefficient for particle velocities. A is the amplitude of the scalar potential at the transducer, placed at the origin of the z_o-coordinate system, at which point the beam width is w_o. This width assumes a value w(d) after propagating a distance d to the interface. The ψ's have similar definitions. A_b is the amplitude of the transmitted potential.

It should be noted that this theory neglects aberrations of the beam, which will become increasingly significant at more oblique angles of illumination. A discussion of the significance of this omission may be found in Ref. 3.

RELATIONSHIP OF GAUSSIAN THEORY TO BEAMS RADIATED BY PISTON TRANSDUCER

The simplicity of the Gaussian beam results creates a temptation to try to apply them to the analysis of beams radiated by more common transducers such as piston sources. Although the radiation of Gaussian and piston sources are distinct, there is enough commonality in certain regimes that the Gaussian theory may provide useful guidelines in the design of NDE systems. The philosophy would be to sacrifice the accuracy of a rigorous piston theory to gain the simplicity of the Gaussian theory and thereby to be able to rapidly examine many configurations. As appropriate, a full theory could be evaluated for special cases of particular interest.

The proper relationship between Gaussian beams and piston sources has been noted in a series of articles by Cook et al. (7-9). Therein, it is noted that the radiation of an ultrasonic beam from any transducer can be approximately described as a superposition of Gaussian-Laguerre or Gaussian-Hermite functions, which are complete orthogonal sets of solutions to the acoustic wave equation in the Fresnel approximation. The first of these functions is the Gaussian beam solution discussed herein. A scale factor, related to the initial beam width w_o in the above analysis, can be freely chosen. For any value of this parameter, the set of functions are complete. However, the rate

of convergence to the solution of a particular problem is dependent on the value selected for the scale factor.

A related approach has been used by Coffey and Chapman (10). They note that the far field radiation pattern of a piston source of radius a, $2J_1(\eta)/\eta$, can be approximately fit by the function $(1-\eta^2/15)\exp(-\eta^2/15)$. Here η represents the angular variable ka sin θ. Their function reproduces the main lobe quite accurately and partially reproduces the first side lobe as is shown in Fig. 2. Coffey and Chapman then employ the Fresnel approximation, and take advantage of the fact that the resulting propagation integrals can be evaluated analytically, to derive an approximate expression for the radiation from a piston source which they feel gives realistic beam structures at axial distances greater than $0.8a^2/z$. Use of trigonometric identities allows their solution to be rewritten as the first two terms of a Gaussian-Laguerre series. However, the coefficients are different from those of Cook's expansion of the piston source radiation, the first two terms of which provide a considerably poorer approximation to the true solution. It can be concluded that a few appropriately chosen Gaussian-Laguerre functions can provide useful beam representations for limited regions of spaces although they do not converge to the correct solution everywhere.

The simplest such approximation is to choose only the first Gaussian-Laguerre function, corresponding to the Gaussian beam whose theory is discussed in this paper, and to use it to represent far field and focussed behavior. In the far field, the piston source radiation has an angular dependence consisting of a main lobe and a series of interference induced side lobes. The far field Gaussian radiation pattern lacks these side lobes. However, in many experiments, the side lobes do not play a primary role. This is particularly true in broadband measurements, since the side lobes at all frequencies do not coherently add. A crude representation of the radiation of a piston source can then be obtained from the radiation of that Gaussian source selected to fit the central lobe in the far field. In this work, the Gaussian parameters have been selected to equalize the two patterns on the beam axis and at 50% of peak amplitude. This leads to the conditions

$$w_o = .7517a \tag{11}$$

$$V_G = 1.770\ V_p \tag{12}$$

where a is the radius of the piston and V_p and V_G are the particle velocities at the centers of the piston and Gaussian, respectively. Accordingly, the Gaussian must be somewhat narrower but with greater peak intensity than the piston source. Figure 2a includes the far field radiation patterns for this approximation as well as the approximation of Coffey and Chapman and the exact theory. Figure 2b compares the axial radiation pattern for the two approximations to the exact case.

When measurements are made in the far field or near a focal point, this Gaussian fit may provide a useful "zeroth order" approximation to the behavior of more commonly used piston sources. The usefulness near focal planes occurs because a lens transforms far

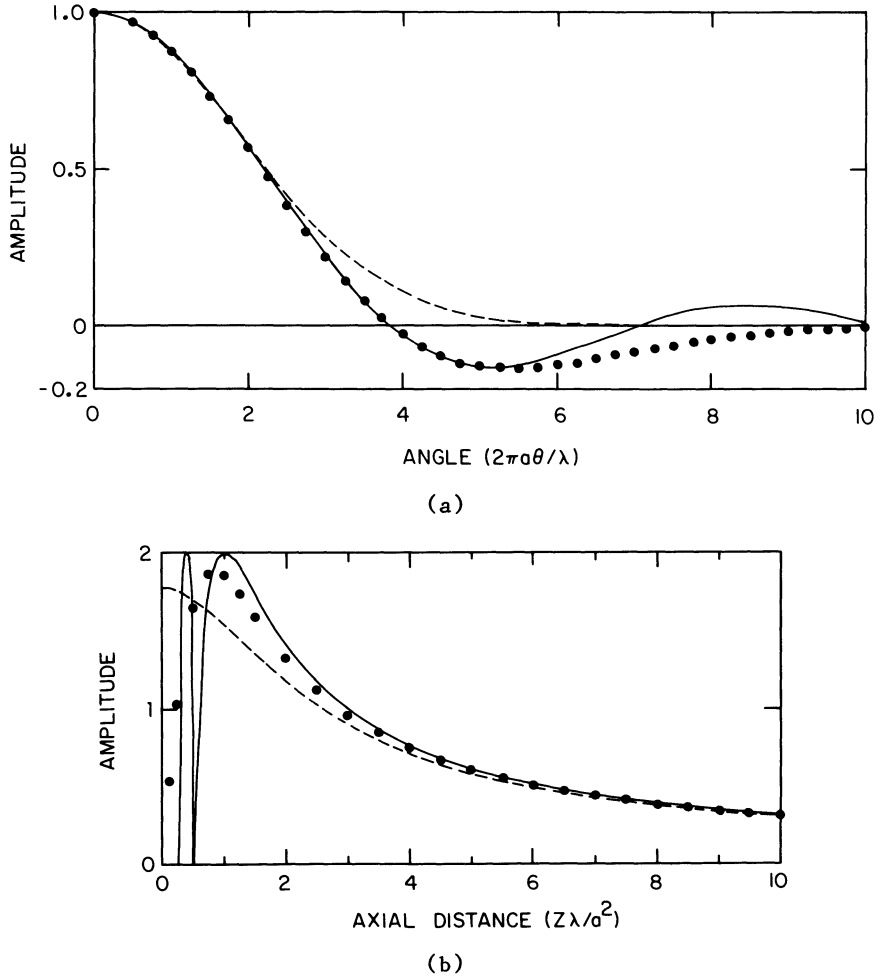

Fig. 2. Comparison of radiation patterns. piston source in Fresnel approximation (——), model of Coffey and Chapman (····), Gaussian fit to central lobe (- - -).

a) far field angular variation. b) axial variation

field behavior to the focal point (11). As examples, Figs. 3 and 4 compare the transverse variation of the radiation of commercially produced transducers to the prediction of the Gaussian beam theory with parameters selected according to Eqs. (11) and (12). Figure 3 compares the theory to data supplied by the manufacturer. For this 10 MHz, 1.9 cm (3/4 in.) diameter probe with a nominal focal length of 10.16 cm (4 in.), the pulse-echo reflection from a planar surface is as shown in the upper portion of the figure. When a small spherical reflector in water (unspecified diameter) was transversely scanned through the focal plane, the peak reflected signal had the

spatial variation shown by the solid line at the bottom of the figure. This is compared to the Gaussian theory at three monochromatic frequencies selected from the transducer spectrum, as indicated by the broken curves. Since a pulse-echo measurement determines the square of the radiation pattern, the theoretical plots are the square of the predicted pressure with w_o determined from Eq. (11) and "a" set equal to the nominal transducer radius. The 7 MHz theory fits the observations well, whereas the 10 and 13 MHz theory predicts a somewhat narrower beam than was observed. Although a direct time domain comparison was impossible since the manufacturer's data did not provide the phase of the transducer spectrum, it seems likely that such a calculation would also produce a beam width less than that observed.

To make a more quantitative comparison, the transverse focal plane scans were repeated in our laboratory (12) for the same transducer, and a second 10 MHz transducer having 1.27 cm (1/2 in.) diameter and the same nominal focal length. In this case, the ultrasound was radiated into water and then passed into an IN100 alloy sample through a planar surface at normal incidence. Pulse-echo reflections from a 0.076 cm (0.030 in.) disk shaped reflector in the focal plane were then recorded and Fourier analyzed to obtain the monochromatic response. The comparison of theory and experiment at the peak frequency of each transducer are shown in Fig. 4. In interpreting these, it must be recalled that, for small numerical apertures, the focal spot size in the solid should be the same as it would have been in the liquid because of the compensating effects of increased numerical aperture and increased wavelength in the solid. The results show that the radiation pattern of the larger diameter probe is about 19% wider than theoretical expectations, as observed previously, while that of the smaller diameter probe is smaller than expected by about 6%. The two sets of data for the larger probe indicate a beam asymmetry. For neither probe were the side lobes expected for a piston source observed. A possible interpretation of these results is that the greater thickness of the lens at its edges caused some attenuation of the amplitude of the signal passing through it. This apodization, which would be more severe at larger transducer diameters (thicker lens at edges), would reduce side lobes and increase beam width in the focal plane. More specific comments cannot be made without a greater data base. In any event, the data fit is considered acceptable in view of the intent to provide a useful "zeroth order" approximation.

Figure 5 shows an example of the application of this technique to predict the response of a scanned inspection. In this case, a 5 MHz, 0.5 inch (1.27 cm) diameter, 4 in. (10 cm) focal length probe was used. The probe was positioned to generate 30° longitudinal waves in a glass sample. The signals were reflected from a 300μm diameter pore located about 1 cm below the glass surface. After adjusting the probe height to produce maximum signal from the flaw, and thereby placing the probe at the focal point, the probe was scanned in the x and y directions, as defined in the inset to Fig. 5. This figure presents the theoretical and experimental contours of equal magnitude of the 5 MHz component of the signal. The agreement between theory and experiment is believed to be excellent. Of particular note is the fact that the elliptical focal spot shape is correctly predicted. The "x" dimensions are larger than the "y" dimensions

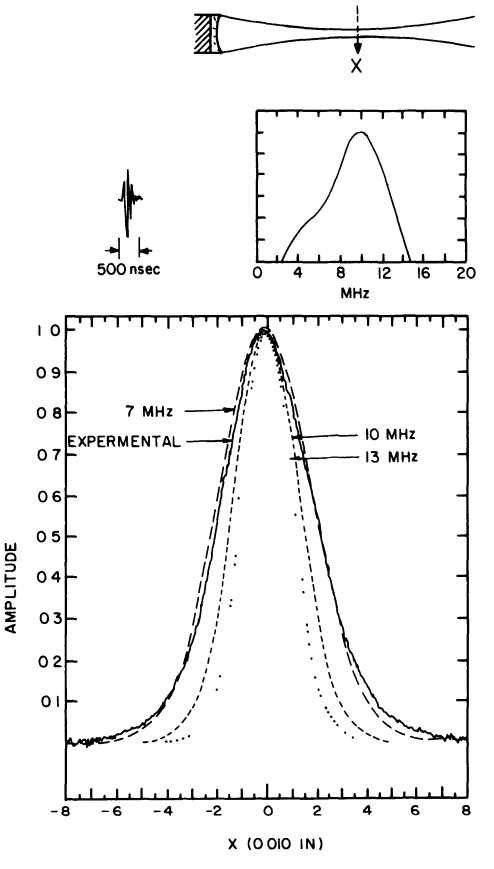

Fig. 3. Comparison of Gaussian fit to measured transverse beam patterns in the focal plane of a 10 MHz, 1.9cm diameter, 10.16cm focal length commercial probe. The time and spectral responses of the probe are shown at the top. The solid curve at the bottom is the variation of the peak pulse-echo response from a small spherical reflector while the broken curves are monochromatic expectations at three frequencies in the pass band.

because the refraction in the x-z plane causes the transducer to have a smaller effective aperture and thus a larger diffraction limited spot size in this plane.

In the near field, the differences between the radiation of the piston and Gaussian sources will be striking (12). Whereas the axial fields of the former exhibit strong interference oscillations for monochromatic excitation, the fields of the latter decrease

monotonically. The Gaussian model should not be used in this regime. Similarly, at large angles of incidence and refractions, the neglect of aberrations in the above analysis limits its accuracy, as discussed in Ref. 3.

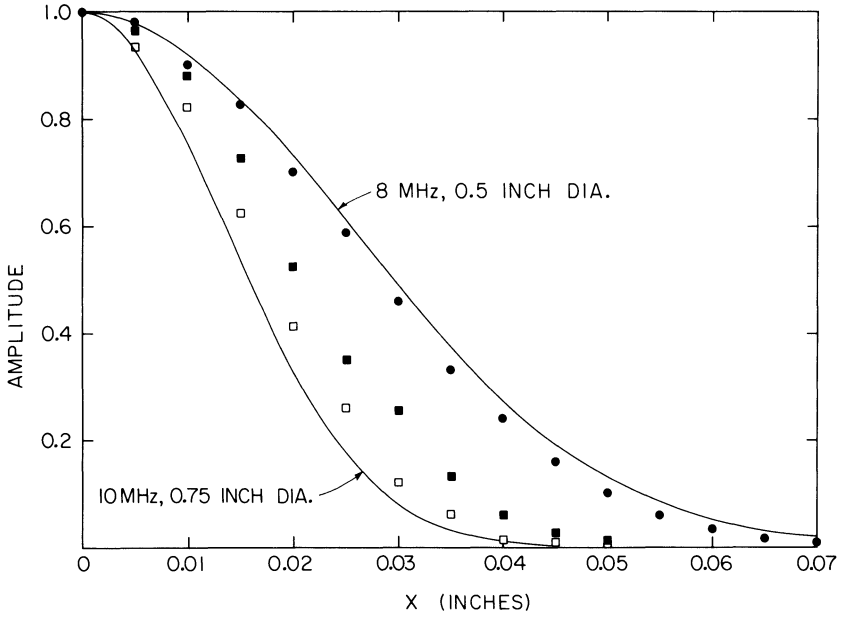

Fig. 4. Monochromatic radiation pattern in the focal plane of two commercial probes with 10.16cm nominal focal length. The solid lines are theoretical predictions and points are measured. A beam asymmetry in the 0.75 inch probe is indicated by two sets of data.

DISCUSSION

A simple theory to describe the propagation of Gaussian ultrasonic beams through lens and interfaces at oblique incidence has been presented. This should be directly useful as Gaussian transducers become more readily available. Furthermore, it provides guidelines for evaluating the effects of diffraction on measurements with piston sources, particularly in the far field or near focal points where interference effects are not dominant.

ACKNOWLEDGEMENT

This work was sponsored by the Center for Advanced Nondestructive Evaluation, operated by the Ames Laboratory, USDOE, for the Air Force Wright Aeronautical Laboratories/Materials Laboratory and the Defense Advanced Research Projects Agency under Contract No. W-7405-ENG-82 with Iowa State University.

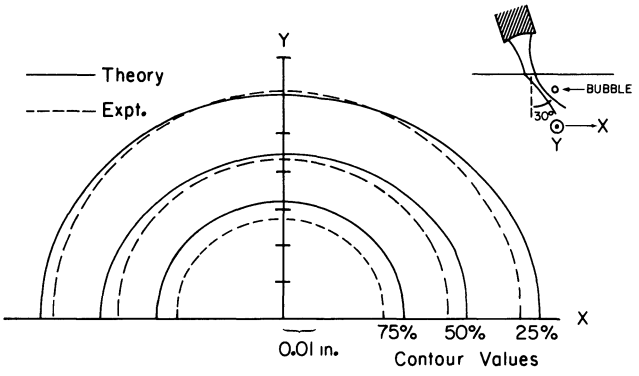

Fig. 5. Comparison of measured and predicted response of a scanned, 30° angle longitudinal scan. The transducer was a 5 MHz, 0.5 in. (1.27 cm) diameter, 4 in. (10 cm) focal length probe. The flaw was a 300μm diameter pore in glass, at a depth of about 1 cm. Transducer height was adjusted to place the pore in the focal plane.

REFERENCES

1. R. T. Beyer and S. V. Letcher, Physical Ultrasonics (Academic Press, New York, 1969), Ch. 1.
2. R. B. Thompson and T. A. Gray, Review of Progress in Quantitative Nondestructive Evaluation 2, D. O. Thompson and D. E. Chimenti, Eds., (Plenum Press, New York, 1983), p. 567.
3. R. B. Thompson and E. F. Lopes, "The effects of focussing and refraction on Gaussian ultrasonic beams", J. of Nondest. Eval. (in press).
4. F. D. Martin and M. A. Breazeale, J. Acoust. Soc. Amer. 49, 1668 (1971).

5. M. A. Breazeale, F. D. Martin, and B. Blackburn, J. Acoust. Soc. Amer. 70, 1791 (1981).
6. R. O. Claus and P. S. Zerwekh, IEEE Trans. on Sonics and Ultrasonics, SU-30, 36 (1983).
7. E. Cavanagh and B. D. Cook, J. Acoust. Soc. Am. 67, 1136 (1980).
8. B. D. Cook and W. J. Arnoult III, J. Acoust. Soc. Am. 59, 9 (1976).
9. Eduardo Cavanagh and Bill D. Cook, J. Acoust. Soc. Am. 69, 345 (1981).
10. J. M. Coffey and R. K. Chapman, Nucl. Energy 22, 319 (1983).
11. J. Goodman, Introduction to Fourier Optics, (McGraw-Hill, New York, 1968).
12. T. A. Gray, R. B. Thompson and B. P. Newberry, "Improvements in ultrasonic measurement modeling with applications to ultrasonic reliability", these proceedings.
13. R. B. Thompson, V. G. Kogan, J. M. Rose, T. A. Gray and E. F. Lopes, 1983 Ultrasonics Symposium Proceedings (IEEE, New York, 1983), p. 905.